AD-A105 442 GEORGIA INST OF TECH ATLANTA FRACTURE AND FATIGUE RE--ETC F/G 7/4
X-RAY SCATTERING INVESTIGATION OF MICROALLOYING AND DEFECT STRU--ETC(U)
AUG 81 S SPOONER N00014-78-C-0270
UNCLASSIFIED GIT-E-19-664 NL

END
DATE
FILMED
0 81
DTIC

Unclassified

SECURITY CLASSIFICATION OF THIS PAGE (When Data Entered)

LEVEL II

14

AD A105442

REPORT DOCUMENTATION PAGE

READ INSTRUCTIONS BEFORE COMPLETING FORM

1. REPORT NUMBER	2. GOVT ACCESSION NO. AD-A105 442
3. RECIPIENT'S CATALOG NUMBER	
4. TITLE (and Subtitle) X-ray Scattering Investigation of Microalloying and Defect Structure in Ion Implanted Copper.	5. TYPE OF REPORT & PERIOD COVERED Progress rept.,
	6. PERFORMING ORG. REPORT NUMBER E-19-664
7. AUTHOR(s) S. Spooner GIT-E-19-664	8. CONTRACT OR GRANT NUMBER(s) N00014-78-C-0270
9. PERFORMING ORGANIZATION NAME AND ADDRESS Fracture & Fatigue Research Laboratory Georgia Institute of Technology Atlanta, GA 30332	10. PROGRAM ELEMENT, PROJECT, TASK AREA & WORK UNIT NUMBERS 26 Aug 81
11. CONTROLLING OFFICE NAME AND ADDRESS Office of Naval Research Department of the Navy, Arlington, VA 22217	12. REPORT DATE August 26, 1981
	13. NUMBER OF PAGES 11 17
14. MONITORING AGENCY NAME & ADDRESS (if different from Controlling Office)	15. SECURITY CLASS. (of this report) Unclassified
	15a. DECLASSIFICATION DOWNGRADING SCHEDULE

16. DISTRIBUTION STATEMENT (of this Report)

Unlimited

DISTRIBUTION STATEMENT A Approved for public release; Distribution Unlimited

17. DISTRIBUTION STATEMENT (of the abstract entered in Block 20, if different from Report)

18. SUPPLEMENTARY NOTES

19. KEY WORDS (Continue on reverse side if necessary and identify by block number)

Ion plating, ion implantation, double-crystal method

20. ABSTRACT (Continue on reverse side if necessary and identify by block number)

The double-crystal method for x-ray scattering analysis of radiation described ~~by B. C. Larson~~ has been applied to the investigation of aluminum implanted copper. The interpretation of x-ray observations is based on effects of lattice strain in the surface microalloy and the presence of dislocation loops which originate from implantation damage. The copper crystal with a dislocation less than 10^3 cm/cm^3 was implanted with aluminum to a dose of 2×10^{16} ions/cm with energies up to 200 keV. The response of the implanted crystal to annealing at 500°C and 600°C was determined. → next page

411C 7

The quantitative use of the x-ray technique to assess implantation effects and the limitations of the technique are discussed.

X-RAY SCATTERING INVESTIGATION OF MICROALLOYING AND DEFECT STRUCTURE IN ION IMPLANTED COPPER

S. Spooner

Fracture and Fatigue Research Laboratory
Georgia Institute of Technology
Atlanta, Georgia 30332

The double-crystal method for x-ray scattering analysis of radiation described by B. C. Larson (1) has been applied to the investigation of aluminum implanted copper. The interpretation of x-ray observations is based on effects of lattice strain in the surface microalloy and the presence of dislocation loops which originate from implantation damage. The copper crystal with a dislocation less than 10^3 cm/cm^3 was implanted with aluminum to a dose of 2 x 10^{16} ions/cm with energies up to 200 keV. The response of the implanted crystal to annealing at 500 C and 600 C was determined. The quantitative use of the x-ray technique to assess implantation effects and the limitations of the technique are discussed.

S. Spooner 1 11

This research was sponsored by the Office of Naval Research under Contract N00014-78-C-0270.

Introduction

X-ray diffraction is an effective method for analyzing radiation damage particularly for quantitative measurement of lattice strain effects associated with defect clusters (1). In recent years there have been a variety of x-ray diffraction investigations of ion implantation damage produced in single crystals based on double-crystal measurements. Komenou et al. (2) observed x-ray scattering Pendellosung interference in rocking curves from Ne^+-implanted garnet films which Speriousu (3) interpreted according to a kinematic diffraction theory incorporating strain and damage distributions as a function of depth. Afanasev et al. (4) have used dynamical theory for calculating the scattering from a silicon crystal with disturbed layers. Yamagishi and Nittono (5) studied Ar^+ ion-implanted copper whiskers with both x-ray topography and a triple-crystal diffraction method to assess lattice strain response with dose and annealing. In the foregoing studies (2-5) no absolute intensity measurements were made so that analysis of structural changes depended mostly upon scattering distribution shape. In the present study, absolute reflectivity measurements are used to study the effects of Al^+-ion damage in copper due to low energy (200 keV) and high dose (2×10^{10} ions/cm) using a double-crystal diffraction method. Both surface alloying and implantation damage are under consideration for their important influence on fatigue crack initiation (6). Because radiation damage production of point defect clusters enters our work in a fundamental way, this paper offers an example of the utility of x-ray scattering techniques in radiation damage research.

The principle challenge in this x-ray study was to find an effective x-ray method for investigating the damage and surface alloying effect in an implanted layer which is much thinner than the sampling depth of x-rays. In addition, there was the consideration of which theoretical analysis of scattering intensity would be most appropriate to describe the combined damage and surface alloying scattering effects. This question was approached from two perspectives; (a) use of dynamical theory of diffraction for the analysis of lattice strain due to surface alloying (7,8) and (b) use of kinematic theory for the description of scattering from defect clusters (1). It is shown that the scattering data are dominated by implantation damage defect clusters and that the kinematic theory is most appropriate for the description of scattering in the case at hand. Furthermore, it is shown that a quantitative evaluation of implantation damage can be obtained from the absolute reflectivity measurements made in the double-crystal method.

X-Ray Scattering Models

The structure the implanted region is modeled by placing of point defect clusters within a surface layer which has a lattice parameter that is expanded by implantation alloying. As yet, no single formulation for scattering intensity gives a calculation of the scattering from the combined defect cluster and lattice distortion effects. Instead, we make a calculation for the case of scattering from a defect-free surface alloy on one hand and a calculation for the scattering from defect clusters in a unalloyed matrix on the other hand. The measured x-ray scattering effects are then used to determine the manner in which the two calculations might be applied to represent the scattering from the implanted layer.

For a surface alloy layer free of defects, the dynamical theory of x-ray scattering can be used to calculate the reflectivity of x-rays as a function of crystal rotation in a double-crystal rocking curve. In a two-crystal arrangement, the first crystal which is not implanted is set to maximum reflectivity. The second crystal is rotated about an axis perpendicular to the scattering plane (defined by the incident and reflected

x-ray beams.) The resulting reflectivity curve is the convolution of the reflection characteristic of the first crystal with the reflectivity of the second crystal. Larson (7,8) has adapted, for this surface alloy problem, a method of calculation used by Klar and Rustichelli (9) for neutron scattering from elastically bent crystals. The reflectivity from a crystal is obtained by the computation of the real and imaginary components of the complex scattering amplitude of the reflected radiation. Two coupled differential equations - one for real and one for imaginary components - are integrated numerically. The integration is dependent upon initial values of the amplitude components and the variation in the Bragg angle for the crystalline sublayers due to the elastic lattice distortion arising from bending or composition change. Full algebraic development of the theory can be found in papers by Larson and Barhorst (8) and Klar and Rustichelli (9). The equations requiring integration express the derivatives of the real (X_1) and imaginary (X_2) scattering amplitude components with respect to a variable A which is proportional to depth measured relative to the external surface:

$$\frac{dX_1}{dA}=k(X_1^2-X_2^2+1)+2X_2(X_1-y)-2gX_1 \qquad (1)$$

$$\frac{dX_2}{dA}=-(X_1^2-X_2^2+1)+2X_1(kX_2+y)-2gX_2 \qquad (2)$$

where k and g are constants which depend on x-ray absorption and the parameter y contains the misset angle, $\Delta\Theta$, for the rocking curve as follows:

$$y=C_1\Delta\Theta-C_2 \qquad (3)$$

where C_1 and C_2 are constants dependent on x-ray scattering parameters tha are fixed for the Bragg diffraction peak under examination. For thr case where the lattice parameter varies with A it is shown (8) that

$$y=C_1(\Delta\Theta+\varepsilon(A)\tan\Theta_B)-C_2 \qquad (4)$$

where the variation of the lattice parameter with depth is contained in the strain function $\varepsilon(A)$. In the case at hand, $\varepsilon(A)$ is determined by the composition of the surface alloy as a function of implantation depth.

The method by which the change in relectivity due to surface alloying is calculated does not require integration over the entire crystal thickness. Instead, one uses the well known results (10,11) for the reflectivity from a perfect crystal as a starting point. The real and imaginary components of the scattering amplitude at a set rocking angle are used as initial values for the integration beginning at a depth below the implanted ions. For the integration back to the surface the effects of surface alloying, $\varepsilon(A)$, are allowed to affect the computation of scattering amplitude. A set of these calculations is done for a range of rocking angles where the reflectivity is calculated from,

$$R(\Delta\Theta)=X_1^2+X_2^2 \qquad (5)$$

where the amplitude components, X_1 and X_2 are evaluated at the reflecting crystal surface. Note that the result is an absolute reflectivity value.

Figure 1 shows the calculated results we have obtained at the reflecting in which 2 atomic percent of aluminum is implanted in copper to a depth of approximately 1000 A. The lattice parameter expansion used in the calculation was taken from the data given on linear lattice strain by King (12) equal to +0.0626 per atomic percent of aluminum in copper. A sharp

subsidiary peak of 1.4 percent reflectivity is seen at a Bragg angle displaced to a lower angle than the substrate Bragg angle corresponding to the expanded lattice parameter. The small peak width is approximately 2 minutes of arc. The reflectivity is the order of the ratio of implanted layer thickness to the x-ray penetration thickness, $1/2\mu_o$, where μ_o is the linear absorption parameter.

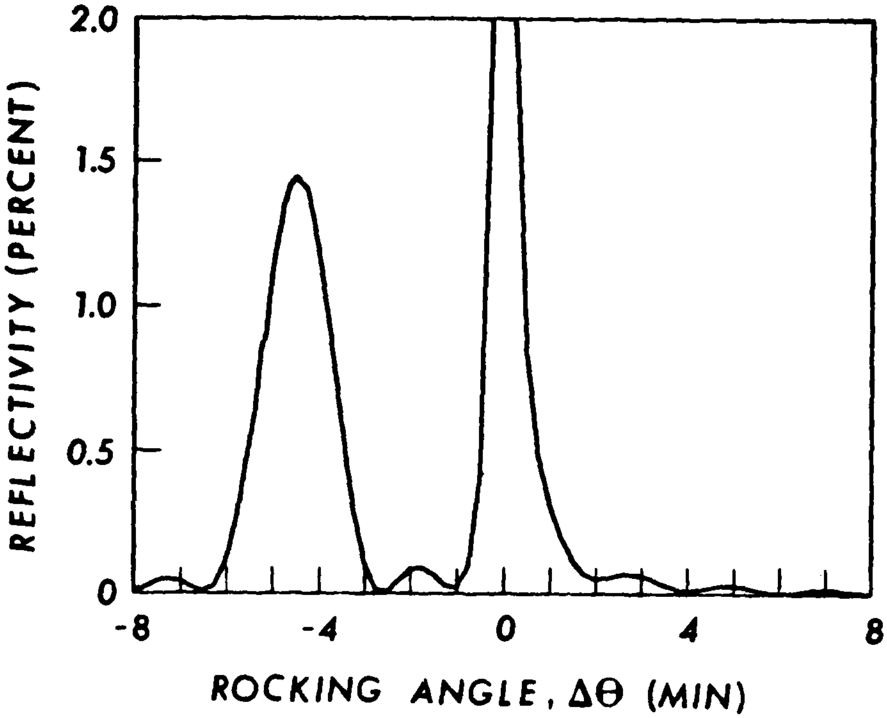

Fig. 1 Calculated reflectivity from a surface implanted to 2 atomic percent of aluminum in copper to a depth of approximately 1000 A The subsidiary peak appears at an angle appropriate for the lattice parameter of this composition.

Consider now the calculation of the scattering from defect clusters in a crystal of uniform lattice parameter. In this case, kinematic diffraction theory is used to calculate the scattering intensity from an isolated defect cluster. The scattering resulting from a collection of defects is the sum of the intensities. This implies that no scattering interference occurs between scattering amplitudes coming from each defect. Larson (1) summarizes the calculation of the scattering intnsity from defect clusters. The experimental geometry used in our experiments is shown in Figure 2 where the scattered x-rays are recieved by a large detector. Each of the scattering vectors is associated with a scattering space vector, q, going from the Bragg spot (at the top) to the surface of the Ewald scattering sphere. In such an experiment, the intensity is averaged over the scattering space vectors, q. q_o is the shortest vector between the Bragg position and the Ewald sphere at a given crystal setting. The measured intensity is called the integral diffuse scattering. The intensity is measured as a function of rocking angle of the crystal in the same geometry used for measurement of dynamical difraction effects described above.

The diffuse scattering from dislocation loops measured close to the Bragg peak is attributed to long range strain fields around the loop and is called Huang scattering. Scattering measured farther away from the Bragg

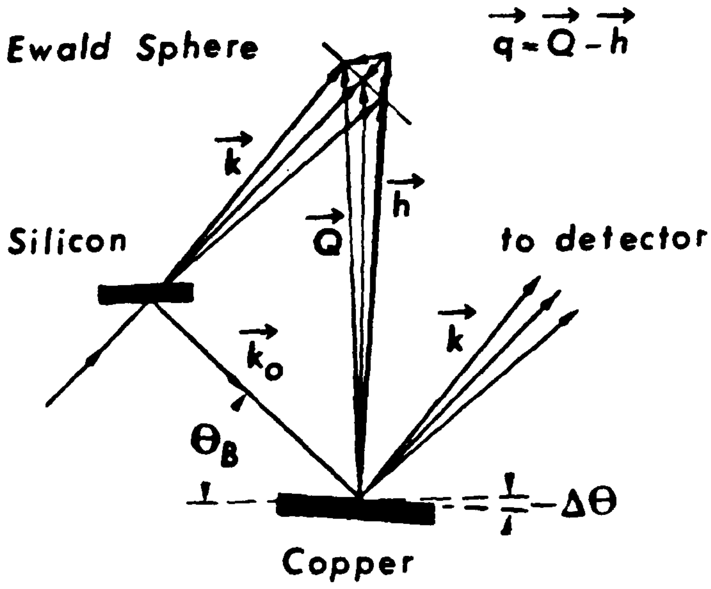

Fig. 2
Scattering geometry for the double crystal method used in this experiment. Upon rocking the crystal the Ewald scattering sphere is swept through the Bragg point. At a fixed crystal setting the diffuse scattering is integrated over a portion of the scattering sphere near the Bragg point.

peak is attributed to short range strain fields and is termed Stokes- Wilson scattering. The diffuse scattering is distributed about the Bragg position in a way dependent on the precise strain field distribution (1,13). The calculation of integral diffuse scattering requires an averaging of the diffuse scattering over the portion of the Ewald scattering sphere which is close to the Bragg position (14). For the scattering from loops of radius R, the Huang scattering smoothly joins the Stokes-Wilson scattering at a scattering parameter $q_o \approx q_L = \alpha/R$ where $q_o = h\Delta\theta\cos\theta_B$ with d_{hk} spacing, $h = 2\pi/d_{hkl}$, θ_B the Bragg angle for reflection from the hkl planes, $\Delta\theta$, the misset angle of the rocking curve. A symmetric diffuse scattering cross section is defined

$$\sigma_h^s(q_o) = 1/2(\sigma_h^s(-q_o) + \sigma_h^s(q_o)) \tag{6}$$

which is obtained by the average of intensities measure symmetrically above and below the Bragg position ($q_o = 0$). The symmetric diffuse cross sections for Huang and Stokes-Wilson scattering are given by,

(Huang) $$\sigma_h^s(q_o) = (r_e^2 f_h^2 e^{-2M}(h/k)^2 2\pi\tau(b\pi R^2/V_c)^2 \ln(e^{1/2} q_L/q_o) \tag{7}$$

for $q_o < q_L$, and,

(Stokes-Wilson) $$\sigma_h^s(q_o) = (r_e^2 f_h^2 e^{-2M}(h/k)^2 2\pi\tau(b\pi R^2/V_c)^2 q_L^2/2q_o^2 \tag{8}$$

for $q_o > q_L$, r_e is the Thompson electron radius (2.82×10^{-13} cm), f is the scattering factor, e^{-M} is the Debye-Waller factor, $k = 2\pi/\lambda$, λ= wavelength, is a constant of order 1 which depends on averaging of loop orientations, b= Burgers vector, V_c= atomic volume, The scattering intensity relative to the incident intensity is given by,

$$\frac{I^s(q_o)}{I_o} = \frac{C(R)}{2\mu_o V_c} \sigma_h^s(q_o) \tag{9}$$

where $C(R)/V_c$ is the density of loops of radius R. From Eqns. (7),(8) and (9) one can obtain loop size and density. Note that $(b\pi R^2/V_c)$ equals the number of point defects in the defect cluster.

In summary of the two calculations, the dynamical theory predicts a subsidiary peak which appears at an angle determined by the lattice strain due to alloying. The kinematic theory predicts a diffuse scattering which is proportional to the number and size of loops. Both calculations give the absolute relectivity with no adjustable parameters other than those describing the structure. The dynamical theory calculation depends on the assumption that the surface alloy is crystallographically coherent with the unalloyed crystal. The kinematic theory is likely to be limited in the case of very high defect cluster densities where nonrandom loop distributions may lead to interference between diffuse scattering amplitudes.

Experimental

The calculated strain scattering effects must be measured at small angles near the Bragg diffraction peak of the unaffected crystal. The implant affected region is less than 1 micron and the penetration depth is approxmately 1/2 = 11 microns. It is required that the bulk of the crystal be perfect (mosaic spread less than 1 minute) in order that the small scattering effects can be measured near the Bragg peak. Furthermore, it is required to subtract a significant background due to the tails of the bulk crystal Bragg peak in order to determine the diffuse scattering intensity due to surface alloying and defect clusters. A convenient approach to this measurement is to translate the crystal between an implanted and implantation-free area on the same crystal. Crystals used in these studies were provided by F. W. Young of Oak Ridge National Laboratory. The crystals were grown by the Bridgeman technique, cut to orientation, then annealed at a few degrees below the melting point for two weeks. The crystal pieces were hardened by neutron irradiation and then further cut and shaped by chemical cutting methods (15). The dislocation density measured by etch pit techniques was less than 10^3 cm^{-2} after shaping procedures were completed.

The two-crystal arrangement consisted of a silicon crystal fixed to diffract the Cu K_α radiation onto the implanted copper crystal. The (333) d-spacing (1.0451 A) of silicon happens to match the (222) d-spacing (1.0436 A) of copper very well so that the system is well focussed to give a narrow rocking curve width. The copper crystal is initially aligned to give a sharp maximum in the rocking curve by adjusting the (111) normal about an axis in the scattering plane. When properly adjusted, the full width at half-maximum (FWHM) of the copper rocking curve is 12.5 arc-seconds. The crystal is mounted on a goniostat which can be translated in the plane of the crystal surface so that rocking curves can be made from the implanted area and masked implantation-free areas. In a typical run, the copper crystal is rocked about an axis perpendicular to the scattering plane at a rate of 5 to 20 arc-seconds per minute while x-ray intensities are recorded continuously at 10 second intervals. The x-ray detector has an active receiving area of 5 cm^2 at a distance of 8 cm so that the subtended solid angle (0.08 steradians) integrates the scattering over a large portion of the Ewald sphere in the vicinity of the 222 Bragg peak of copper.

The implantation of aluminum into copper was chosen for these experiments because the ion penetration was favorable and the microalloy concentration was well below the solubility limit of the aluminum in copper. The details of implantation are given elsewhere (19). The implanted layer was 1200 A thick (16) with a composition of 1.8 atomic percent. The distribution of damage over the alloy thickness was estimated on the basis of calculations by Fritzsche (17) and Winterbon (18). The alloy distribution (solid line) and the damage profile (dashed line) are shown in Figure 3.

Fig. 3
Distribution of implanted Al^+ ions (solid) and the energy deposition (dashed) for the implantation of $2x10^{16}$ ion/cm^2 with energies up to 200 keV. Note that damage is concentrated toward the surface and that the damage energy is on a relative scale.

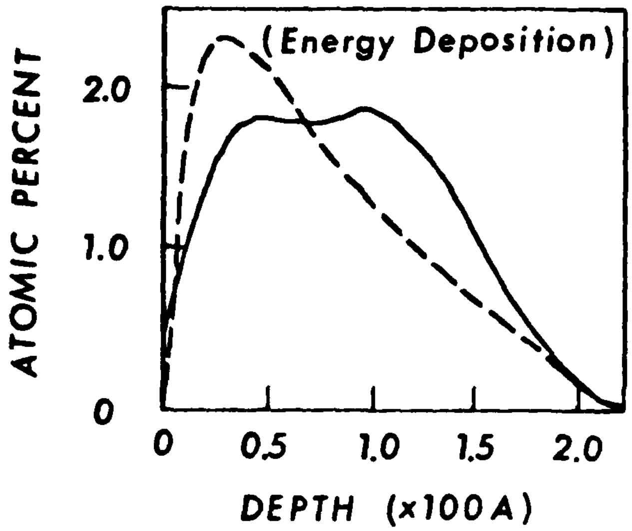

Annealing of the specimens was performed as a means to differentiate the sources of scattering in the implanted layers. The crystals were placed in a vacuum of 10^{-8} Torr at 500 C, 600 C and 900 C for 30 minutes. Annealing at 900 C restored the original structure as seen in the rocking curves.

Fig. 4
Rocking curves are shown for the implanted (upper) and implantation-free (lower) crystal. The scattering is expressed as a fraction of the incident beam intensity. Note the larger scattering at low angles.

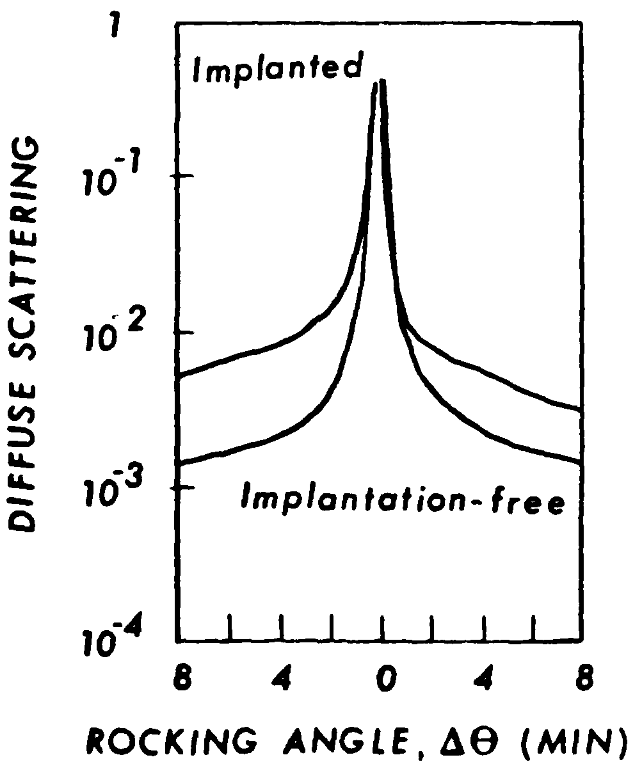

Fig. 5
Excess diffuse scattering intensity for the sample before annealing (dashed) and after annealing (solid) at 500 C. Note that little change in the general level and distribution of the excess intensity occurs upon annealing.

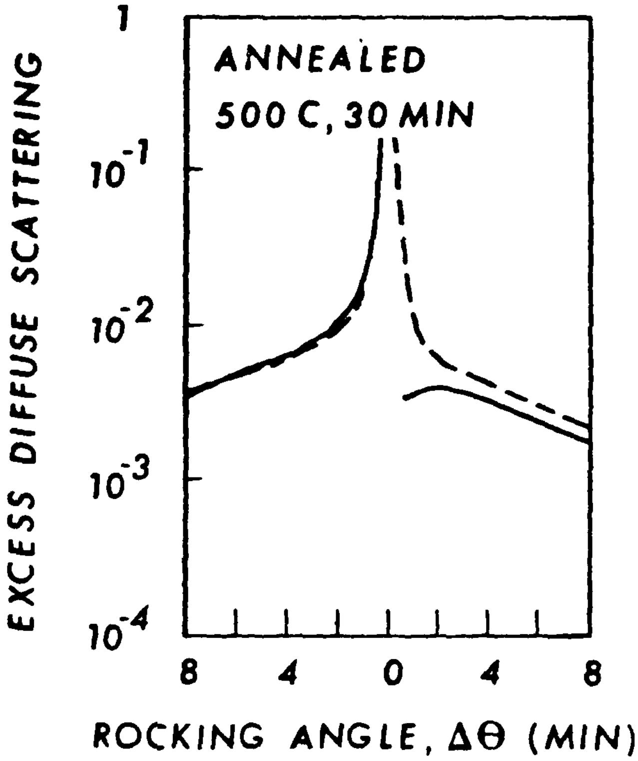

Fig. 6
Excess diffuse scattering intensity for the sample before annealing (dashed) and after annealing (solid) at 600 C. The level and the distribution of the excess intensity changes as a result of the annealing at this temperature.

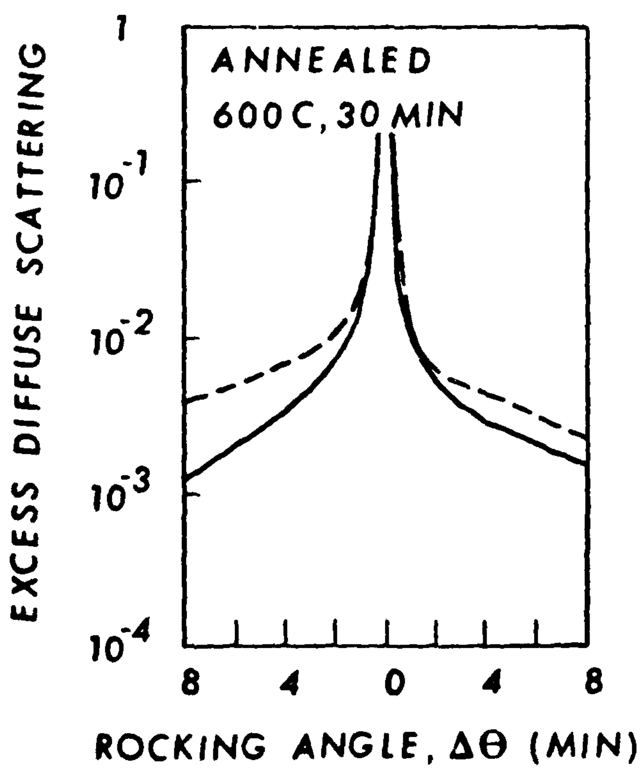

Results and Discussion

The rocking curves for implantation-free copper and for aluminum implanted copper were measured on the same crystal. These curves are shown in Figure 4. The diffuse scattering from the implanted crystal is more intense on the low angle side of the Bragg peak position. The excess diffuse scattering is calculated by subtraction of the implantation-f ee rocking curve intensity from the corresponding intensity in the implanted crystal. The excess diffuse scattering for the implanted crystal is shown in Figures 5 and 6 as a dashed line. The effect of 30 minute anneals on the excess diffuse intensity is show in Figure 5 for annealing at 500 C and in Figure 6 for annealing at 600 C. No large change due to annealing occurs at 500 C while for annealing at 600 C, there is a reduction of scattering and scattering becomes more symmetric with respect to the Bragg peak position.

The observation of a higher diffuse scattering at low rocking curve angles can be attributed to the fact that implanted aluminum expands the copper lattice so that Bragg scattering from the implanted region occurs at a lower angle than that for the implantation-free material. The composition of the implanted layer was estimated to be 1.8 atomic percent. The resulting Bragg position would be displaced to lower angle by 4.2 minutes for the 222 reflection from the copper alloy layer.

The diffuse scattering seen on both sides of the main Bragg position can be compared to calculations of the scattering from dislocation loops. In Figure 7 the excess diffuse scattering is plotted versus the log of the rocking angle according to Eqn. (7) for Huang loop scattering. The rocking angle was measured relative to the supposed Bragg position for the alloy.

Fig. 7
The excess diffuse scattering from the implanted crystal is plotted versus $\ln(\Delta\theta)$ for the intensity above and below the Bragg position assumed to apply for the implanted region of the crystal.

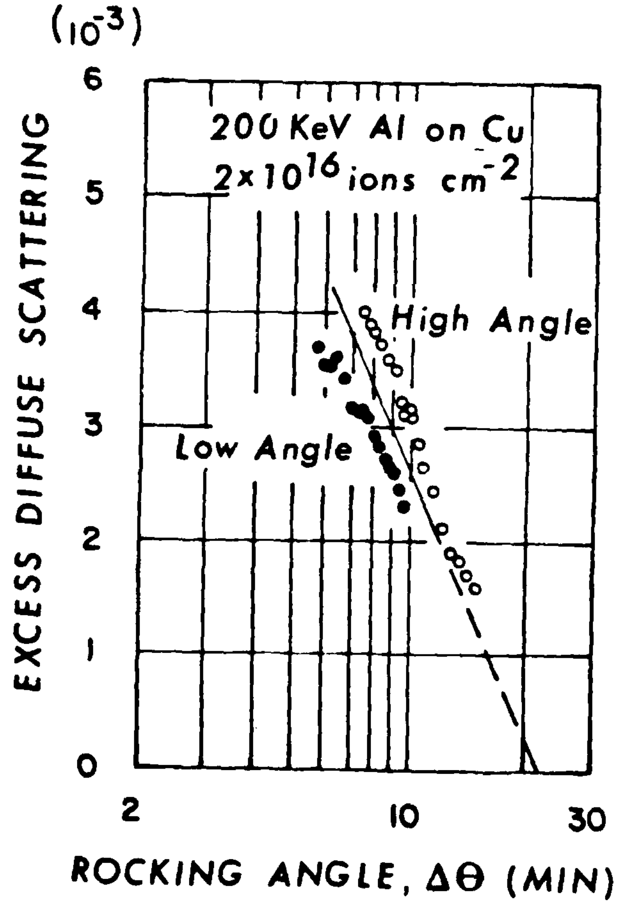

Although there is a displacement between the two sets of points, the average of the high angle and low angle intensity is close to a straight line which yields an estimated loop radius of 25 A.

An estimate of the density of loops can be made by comparing measured reflectivity with Eqn. (9). We use a loop radius of 25 A and a reflectivity of 1 percent at $\Delta\theta = 2$ minutes. Substitution of appropriate constants into Eqn. (9) for a 25 A loop size gives

$$\frac{I^s(q_o)}{I_o} = 6.1\times10^{-21}\frac{C}{V_c}\ln\left(\frac{44}{\Delta\Theta(\mathrm{min})}\right) \tag{10}$$

from which a value of C/V_c is 5.3×10^{17} loops/cc. (The loops are concentrated by a factor of 40 in the implanted layer since the above calculation assumes the loops to be uniformly distributed).

The failure to observe a sharp Bragg peak associated with the implanted aluminum and the general agreement with scattering levels calculated for loop scattering point to the conclusion that the kinematic theory for diffraction from an implanted crystal containing loops is appropriate. The annealing at 600 C produces symmetrical scattering which suggests that most of the aluminum is removed from the region where loops persist. Thereby the loop scattering now originates in essentially pure copper. The role of aluminum is seen as simply expanding the lattice in a region where loops persist which, by virtue of severe damage, is no longer strictly coherent with the implantation-free crystal.

Conclusions

Analysis of x-ray diffraction in aluminum-ion implanted copper suggests that defect cluster scattering dominates the observed rocking curve intensity. Alloying in the implanted layer contributes through a shifting of the diffuse scattering to lower angles due to the fact that the defect clusters are formed in a region of aluminum-expanded lattice. The formation of a distinct peak predicted by dynamical diffraction theory does not occur, probably because of the intense defect scattering and the widths of the peak from the thin layer. Problems in the analysis of scattering remain in the area of formulating a model of combined alloying and defect cluster scattering as well as description of very high defect cluster scattering. Nevertheless the simplistic interpretation of x-ray scattering observation provides useful insights into the type and quantity of damage as well as the annealing response of the implanted structure. Measurements carried out to larger q_o will be useful in further definition of the defect structure since Bragg scattering from the implantation-free and implanted layer are avoided and the kinematical theory can be assumed. Size distributions an and total point defect densities are more directly measurable at the larger q_o values (1) as well.

Acknowledgements

The author thanks Dr. B. C. Larson and Mr. Jim Barhorst of the Solid State Division of Oak Ridge National Laboratory for their considerable help in the collection of the data and many useful discussions.

References

1. B. C. Larson, "X-ray Studies of Defect Clusters in Copper," J. Appl. Cryst. , 8 ,pp. 150-160 (1975).

2. K. Komenou, I. Hirai, K. Asama and M. Sakai, "Crystalline and Magnetic Properties of an Ion-Implanted Layer in Bubble Garnet Films," J. Appl. Phys. , 49 ,pp. 5816-5822 (1978).

3. V. S. Speriousu, H. L. Glass and T. Kobayashi, "X-ray Determination of Strain and Damage Distributions in Ion-Implanted Layers," Appl. Phys. Lett. , 34 , pp. 539-542 (1979).

4. A. M. Afanasev, M. V. Kovalchuck, E. K. Kovev and V. G. Kohn, "X-ray Diffraction in a Perfect Crystal with Disturbed Surface Layer," Phys. Stat. Sol. (a) 42 , pp. 415-422 (1977)

5. H. Yamagishi and O. Nittono, "X-ray Study on Lattice Defects in Ar^+ Ion Implanted Copper Whiskers," Nip. Kinz. Gakk. , 43 , pp. 689-695 (1979).

6. A. Kujore,S. B. Chakrabortty and E. A. Starke, "The Effect of Ion Implantation on the Fatigue Properties of Polycrystalline Copper," Nucl. Instr. Meth., 182/183, pp. 949-958 (1981).

7. B. C. Larson, C. W. White and B. R. Appleton, "Unidirectional Contraction in Boron-Implanted Laser-Annealed Silicon," Appl. Phys. Lett., 32, pp. 801-803 (1978).

8. B. C. Larson and J. F. Barhorst, "X-ray Study of Lattice Strain in Boron Implanted Laser Annealed Silicon," J. Appl. Phys., 51, pp.3181-5 (1980).

9. B. Klar and F. Rustichelli, "Dynamical Neutron Diffraction by Ideally Curved Crystals," Nuovo Cimento, 13B, pp. 249-270 (1973).

10. B. E. Warren, X-ray Diffraction, Chapter 14, pp. 315-354, Addison-Wesley Press, Reading, Mass. (1969).

11. W. H. Zachariasen, Theory of X-ray Diffraction in Crystals, Chapter 3, pp. 83-155, Dover Publications, New York (1967).

12. H. W. King, "Quantitative Size-Factors for Metallic Solid Solutions," J. Mat. Sci, 1, pp. 79-90 (1966).

13. B. C. Larson and W. Schmatz, "Huang-Diffuse Scattering from Dislocation Loops and Cobalt Precipitates in Copper," Phys. Rev. , B10, pp. 2307-2314 (1974).

14. B. C. Larson and F. W. Young, Jr. , "A Comparison of Diffuse Scattering by Defects and Measured in Anomalous Transmission and Near Bragg Reflections," Z. Naturforsch. , 28a, pp. 626-632 (1973).

15. F. W. Young, Jr. , "Etch Pit Studies of Dislocations in Copper Crystals Deformed by Bending. I. Annealed Crystals. II. Irradiated Crystals," J. Appl. Phys. , 33, pp. 3553-3564 (1962).

16. J. Keinonen, M. Hautala, M. Luomajari, A. Antilla and M. Bister, "Ranges of $^{27}Al^+$ Ions in Nine Metals Measured by (p,γ) Resonance Broadening," Rad. Eff. , 39, pp. 189-193 (1978).

17. C. R. Fritzche, "A Simple Method for the Calculation of Energy Deposition Profiles from Range Data of Implanted Ions," Appl. Phys. Lett. , 12, pp. 347-353 (1977).

18. K. B. Winterbon, Ion Implantation Range and Energy Deposition Distributions, Vol. 2, Low Incident Ion Energies, Plenum Press, New York (1975)

19. S. Spooner and K. Legg, "X-ray Diffraction Characterization of Aluminum Ion-Implanted Copper Crystals," Ion Implantation Metallurgy, C. M. Preece and J. K. Hirvonen, eds. TMS AIME, pp. 162-170 (1980).

11

DISTRIBUTION LIST

(One copy unless otherwise noted)

(1 copy + balance after distribution)
Mr. Michael D. Valentine
AIR-5163C4
Naval Air Systems Command
Washington, DC 20361

Commander
Naval Air Development Center
(Code 302)
Warminster, PA 18974

Naval Sea Systems Command
(Code 03423)
Department of the Navy
Washington, DC 20360

Naval Ships Research & Development
Center
(Code 2812)
Annapolis, MD 21402

Commander
Naval Surface Weapons Center
(Metallurgy Division)
White Oak
Silver Spring, MD 20910

Director, Naval Research Laboratory
(Codes: 6330, 6490, 6601, 8430 - 1 copy each)
Washington, DC 20390

Office of Naval Research
The Metallurgy Program, Code 471
Arlington, VA 22217

Dr. [illegible] R. McNelley
Dept. of Mechanical Engineering (Code 59)
Naval Postgraduate School
Monterey, CA 93940

14 copies (12 copies for DDC, 2 copies
for AIR-954)
Commander, Naval Air Systems Command
AIR-954
Washington, DC 20361

Wright-Patterson Air Force Base
Ohio 45433
Attn. W. Griffith, AFML/LLS

Wright-Patterson Air Force Base
Ohio [illegible]5422
Attn. C. L. Harmsworth, AFML/[illegible]

Army Materials & Mechanics Research
Center
Watertown, MA 02172
Attn: Dr. A. Gorum

Defense Documentation Center
Cameron Station
Bldg. 5
Alexandria, VA 22314

Douglas Aircraft Company
3855 Lakewood Blvd.
Long Beach, California 90808
Attn: Mr. Fred Mehe, C1-250

Sikorsky Aircraft
Division of United Aircraft Corp.
Stratford, Connecticut 06497
Attn: Materials Dept.

Boeing-Vertol Company
Boeing Center
P. O. Box 16858
Philadelphia, Pa. 19142
Attn: Mr. J. M. Clark

The Boeing Company
Commercial Airplane
ORG. 6-8733, MS77-18
P. O. Box 3707
Seattle, Washington 98124
Attn: Cecil E. Parsons

Northrop Corporation
Aircraft Division
Dept. 3771-62
3901 West Broadway
Hawthorne, California 90250
Attn: Mr. Allen Freedman

Vought Corp.
P. O. Box 5907
Dallas, Texas 75222
Attn: Mr. A. Hohman

McDonnell Aircraft Company
St. Louis, Missouri 63166
Attn: Mr. H. J. Siegel
Materials & Processes Dev.
General Engineering Division

Lycoming Division
AVCO Corporation
Stratford, Connecticut 06497
Attn: Mr. Barry Goldblatt

Detroit Diesel Allison Division
General Motors Corporation
Materials Laboratories
Indianapolis, Indiana 46206

AiResearch Manufacturing Co. of America
Sky Harbor Aircraft
402 S. 36th St.
Phoenix, Arizona 85034
Attn: Mr. Jack D. Tree, Dept. 93-35-5M

General Electric Company
Aircraft Engine Group
Materials & Processes Technology Laboratories
Evendale, Ohio 45215

Solar
2200 Pacific Highway
San Diego, California 92112
Attn: Dr. A. Metcalfe

Teledyne CAE
1330 Laskey Road
Toledo, Ohio 43601

Dr. Charles Gilmore
Tompkins Hall
George Washington University
Washington, D.C. 20006

Dr. Michael Hyatt
The Boeing Company
P. O. Box 707
Seattle, Washington 98124

General Electric Company
Corporate Research & Development
P. O. Box 8
Schenectady, New York 12301
Attn: Dr. D. Wood

Westinghouse Electric Company
Materials & Processing Laboratories
Beulah Road
Pittsburgh, Pennsylvania 15235
Attn: Don E. Harrison

Dr. John D. Wood
Associate Professor
Lehigh University
Bethlehem, Pennsylvania 18015

General Dynamics Corp.
Convair Aerospace Division
Fort Worth Operation
P. O. Box 748
Fort Worth, Texas 76101
Attn: Tom Coyle

Commanding Officer
Office of Ordnance Research
Box CM, Duke Station
Durham, North Carolina 27706

U.S. Army Armament R&D Command
(ARRADCOM)
Dover, NJ 07801
Attn: Dr. J. Waldman
DRDAR-SCM-P, Bldg. 3409

National Aeronautics & Space Administration
(Code RWM)
600 Independence Ave., S.W.
Washington, D.C. 20546

National Aeronautics & Space Administration
Langley Research Center
Materials Division, Langley Station
Hampton, Virginia 23365
Attn: Mr. H. F. Hardrath
Stop 188M

National Aeronautics & Space Administration
George C. Marshall Space Flight Center
Huntsville, Alabama 35812
Attn: Mr. J. G. Williamson
S&E-ASTN-MMC

National Academy of Sciences
Materials Advisory Board
Washington, D.C. 20418
Attn: Dr. J. Lane

Director
National Bureau of Standards
Washington, D.C. 20234
Attn: Dr. E. Passaglia

Battelle Memorial Institute
505 King Avenue
Columbus, Ohio 43201
Attn: Mr. Stephan A. Rubin, Mgr.
Information Operations

IIT Research Institute
Metals Research Department
10 West 35th Street
Chicago, Illinois 60616
Attn: Dr. N. Parikh

General Dynamics Convair Div.
P. O. Box 80847
San Diego, California 92138
Attn: Mr. Jack Christian, Code 643-10

Kaman Aerospace Corporation
Old Windsor Road
Bloomfield, Connecticut 06001
Attn: Mr. M. L. White

Rockwell International
Columbus Division
Columbus, Ohio 43216
Attn: Mr. P. Maynard, Dept. 75
Group 521

Rockwell International
Rocketdyne Division
Canoga Park, California 91305
Attn: Dr. Al Jacobs
Group Scientist
Materials Branch

Rockwell International
Los Angeles Division
International Airport
Los Angeles, California 90009
Attn: Gary Keller
Materials Applications

Lockheed Palo Alto Research Laboratories
Materials Science Laboratory
3251 Hanover Street
Palo Alto, California 94303
Attn: Dr. Frank A. Crossley
52-31/204

Lockheed California Company
P. O. Box 551
Burbank, California 91503
Attn: Mr. J. M. VanOrden
Dept. 74-71, Bldg. 221, Plt. 2

Lockheed-Georgia Company
Marietta, Georgia 30061
Attn: E. Bateh

Lockheed Missile & Space Corp.
Box 504
Sunnyvale, California 94088
Attn: Mr. G. P. Pinkerton
Bldg. 154, Dept. 8122
Mr. C. D. McIntyre
Bldg. 182, Dept. 84-13 (1 each)

Dr. A. I. Mlavsky
Senior Vice President for Technology &
Director of Corporate Technology Center
Tyco Laboratories, Inc.
16 Hickory Drive
Waltham, Massachusetts 02145

Martin Marietta Aluminum
Attn: Mr. Paul E. Anderson
(M/C 5401)
19200 South Western Avenue
Torrance, California 90509

Dr. Howard Bomberger
Reactive Metals, Inc.
Niles, Ohio 44446

Mr. W. Spurr
The Boeing Company
12842 72nd Ave., N.E.
Kirkland, Washington 98033

Dr. John A. Schey
Department of Materials Engineering
University of Illinois at Chicago Circle
Box 4348
Chicago, Illinois 60680

Rockwell International
P. O. Box 1082
1027 Camino Dos Rios
Thousand Oaks, California 91320

Pratt & Whitney Aircraft
Division of United Technologies
Florida Research and Development Center
P. O. Box 2691
West Palm Beach, Florida 33402

P. R. Mallory & Co., Inc.
3029 East Washington Street
Indianapolis, Indiana 46206
Attn: Technical Librarian

Martin Marietta Corporation
P. O. Box 5837
Orlando, Florida 32805
Attn: Dr. Richard C. Hall
Mail Point 275

Southwest Research Institute
8500 Culebra Road
P. O. Box 28510
San Antonio, Texas 78284
Attn: Dr. C. Gerald Gardner

Avco Space Systems Division
Lowell Industrial Park
Lowell, Massachusetts 01851

Brush Wellman, Inc.
17876 St. Clair Avenue
Cleveland, Ohio 44110
Attn: Mr. Bryce King

General Electric
Missile & Space Division
Materials Science Section
P. O. Box 8555
Philadephia, Pennsylvania 91901
Attn: Technical Library

Kawecki Berylco Industries
P. O. Box 1462
Reading, Pennsylvania 19603

Linde Company
Division of Union Carbide
P. O. Box 44
Tonawanda, New York 14152

Midwest Research Institute
425 Volker Boulevard
Kansas City, Missouri 64110

University of California
Lawrence Radiation Laboratory
P. O. Box 808
Livermore, California 94550
Attn: Mr. L. W. Roberts

ERDA Division of Reactor Development
and Technology
Washington, D.C. 20545
Attn: Mr. J. M. Simmons, Chief
Metallurgy Section

Dr. W. C. Setzer, Director
Metallurgy & Surface Technology
Consolidated Aluminum Corp
P. O. Box 14448
St. Louis, MO 63178

Kaiser Aluminum & Chemical Corp.
Aluminum Division Research Center
for Technology
P. O. Box 870
Attn: T. R. Pritchett
Pleasanton, CA 94566

Reynolds Metals Company
Metallurgical Research Division
4th & Canal Streets
Richmond, VA 23219
Attn: Dr. J. H. Dedrick

The Dow Metal Products Company
Hopkins Building
Midland, MI 48640

Dr. F. N. Mandigo
Olin Metals Research Laboratories
91 Shelton Ave
New Haven, CT 06515

General Electric Co
Corporate Research & Development
Bldg. 36-441
Schenectady, NY 12345
Attn: Dr. J. H. Westbrook, Manager
Materials Information Services

Dr. E. A. Starke, Jr.
[illegible] of Chemical Engineering & Metallurgy
[illegible] Institute of Technology
[illegible], GA 30332

[illegible], Chairman
[illegible] of Materials Science & Engineering
[illegible]
[illegible] University
[illegible] NY 14853

[illegible] J. Duquette
[illegible] Engineering Dept.

[illegible], NY 12181

[illegible] Technologies Research Laboratories
[illegible]ford, CT 06108
[illegible] Mr. Roy Fanti

Autonetics Division of Rockwell
International
P. O. Box 4173
Anaheim, CA 92803
Attn: Mr. A. G. Gross, Jr.
Dept. 522-92